Supplementary Materials

Supplementary figures

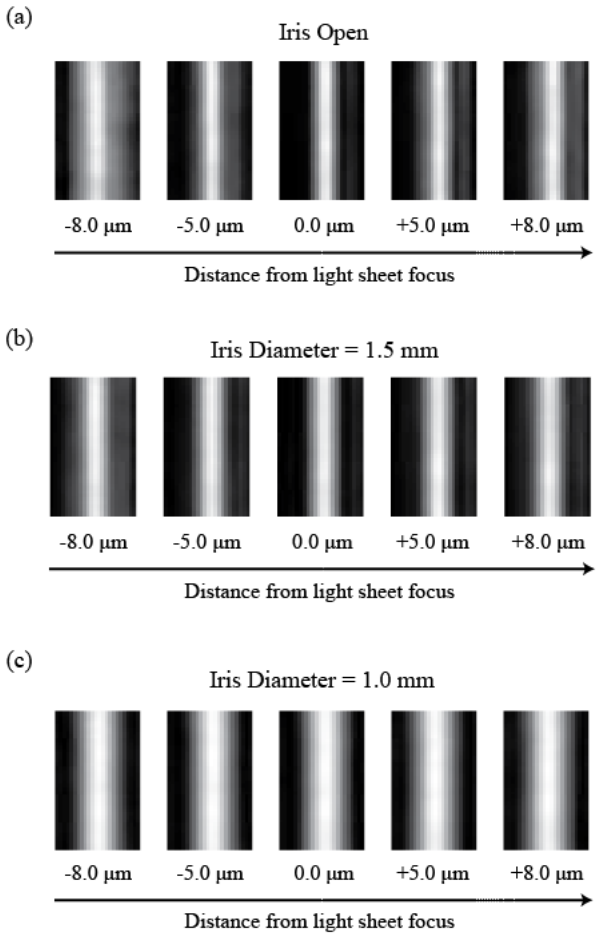

Fig. S1 Calibration of ImTLSM illumination profile. (a), (b), (c) FWHM of light sheet as a function of the distance from the focus. Light sheet profile images were taken using EMCCD directly under weak 561 nm laser illumination, with detection objective scanned along *z*-axis. (a) Iris all open (iris diameter = ∞). (b) Iris diameter = 1.5 mm. (c) Iris diameter = 1.0 mm (Pixel size: 262 nm)

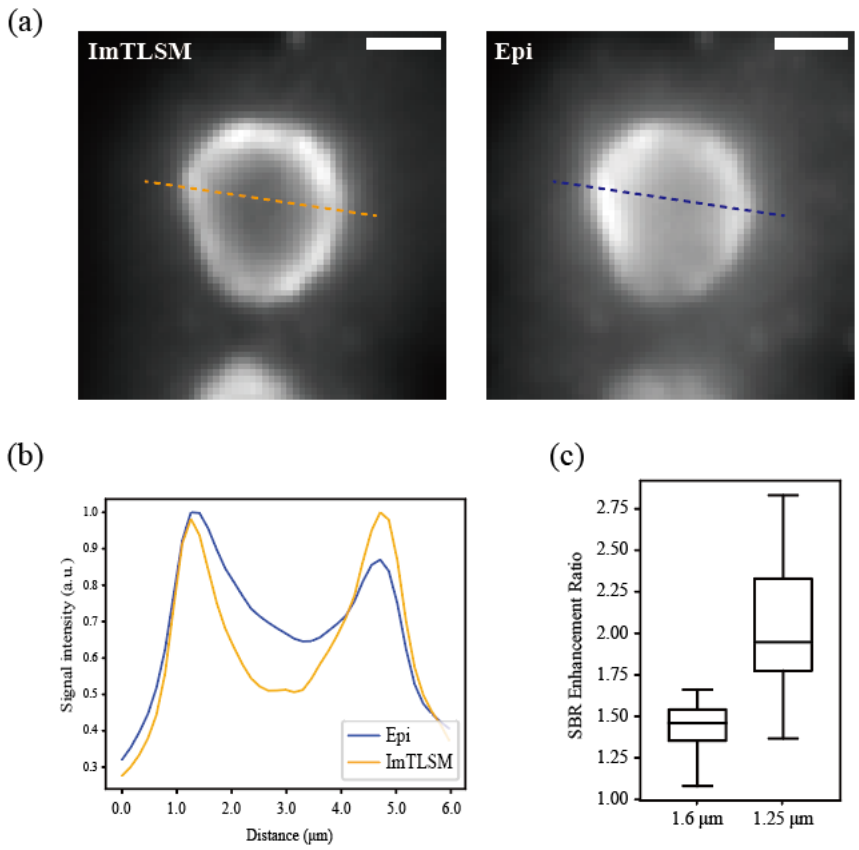

Fig. S2 (a) Immuno-fluorescently labelled NCL protein distribution. Images were taken under different illumination modes (left: ImTLSM (iris diameter =1.5 mm), right: epi-illumination, scale bar: 2 μm). (b) Intensity profile from dashed lines on (a) (orange solid line: ImTLSM, blue solid line: epi-illumination). The SBR enhancement is about 1.3 folds in the picture. (c) Statistic comparison under different light sheet beam waists (1.6 μm for iris diameter 1.5 mm, 1.25 μm for iris all open). The SBR here was defined as the averaged signal intensity from four maximum intensities along radial direction divided by averaged intensity in the center of each image. Each box plot was calculated from 30 different cells. The relatively large standard deviation mainly resulted from the diversity of nucleolus shape

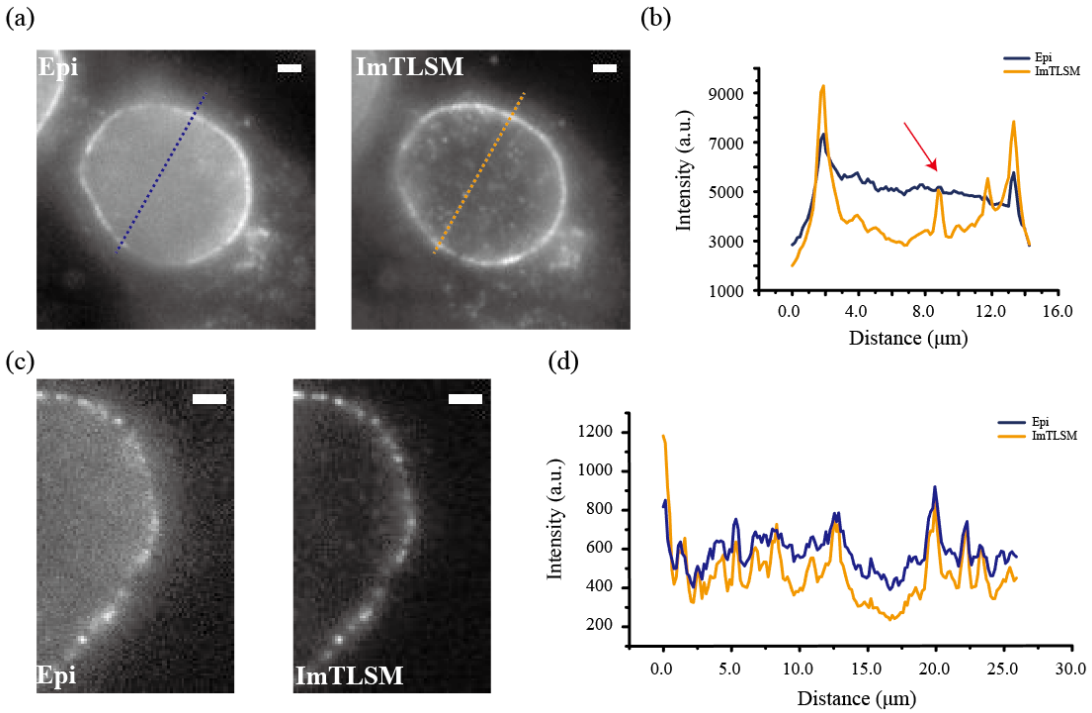

Fig. S3 Comparison between ImTLSM illumination mode ((a) and (c) right) and epi-illumination ((a) and (c) left). (a) Lamin B1 sample. (b) Intensity comparison along the dashed line under different illumination modes in (a), red arrow indicates the outstanding SBR enhancement for single-molecule signal. (c) Nup133 sample. (d) Intensity comparison along the edge of nuclear in (c). It was clear that the weak fluorescence points that were obscured by the high background could be resolved under ImTLSM illumination (Scale bar = 2 μm)

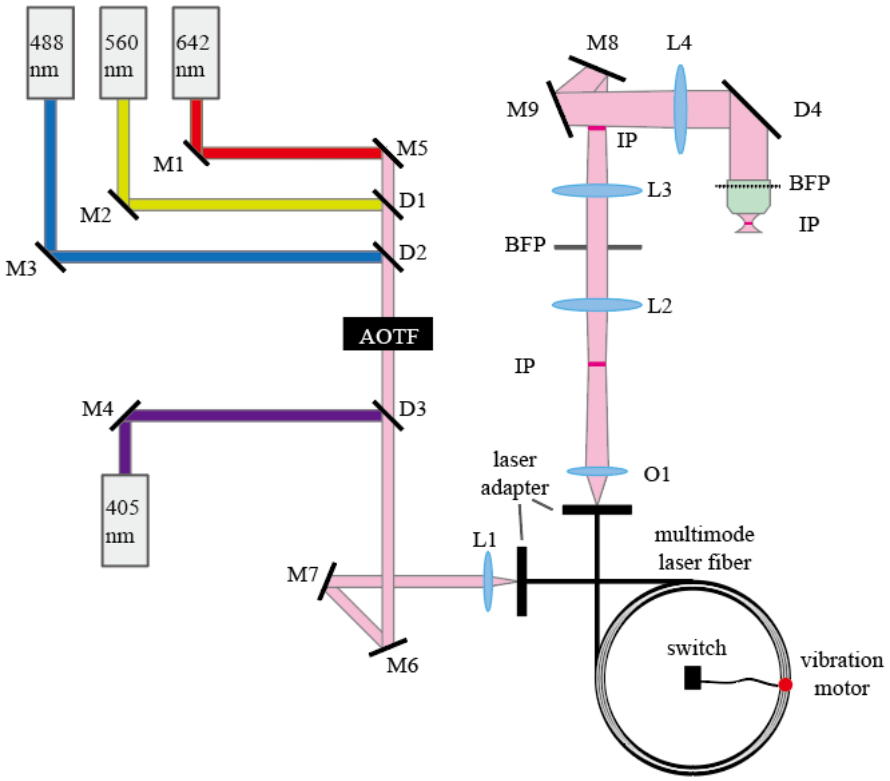

Fig. S4 Optical path for large-field illumination. M1–M9: aluminum mirrors (Thorlabs); D1–D4: dichroic mirror; O1: objective (10×/NA0.25, Olympus); L1: lens (AC050-010-A-ML, Thorlabs); L2 and L3: lens (AC254-75-A-ML, Thorlabs); L4: lens (AC254-250-A-ML, Thorlabs); BFP: back focal plane; IP: imaging plane. We used Eclipse Ti-E (Nikon) microscope and DU-897D (Andor) EMCCD. The fiber (WFANS 200 × 200 / 238 × 238, CeramOptec) was specially designed to generate large-field illumination

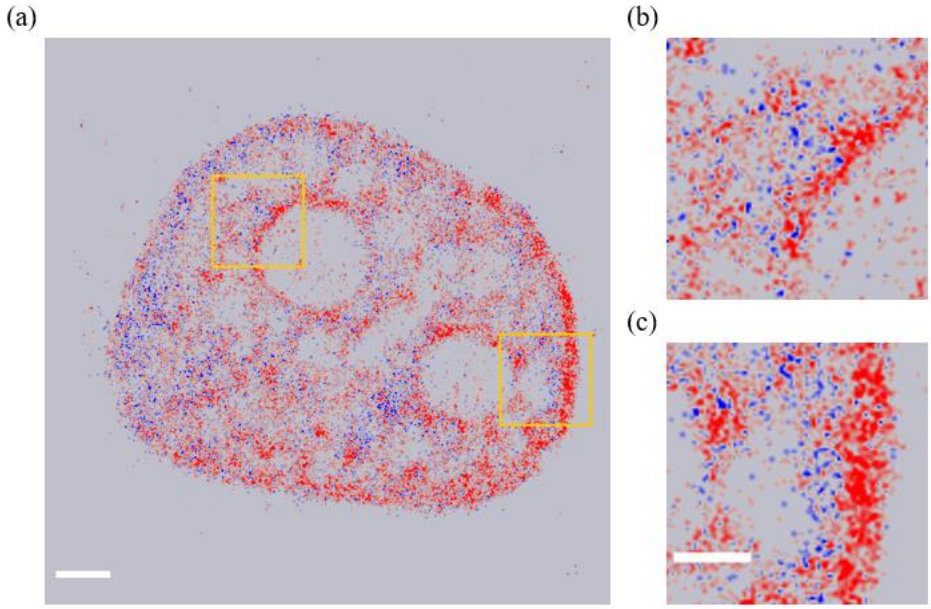

Fig. S5 Difference between SMLM images obtained by PN-ImTLSM and the conventional method. (a) Red pixels are pixels where PN-ImTLSM identified more localizations than the conventional method, and blue pixels are pixels where the conventional method identified more localizations than PN-ImTLSM (scale bar: 2 μm). (b) Enlarged ROI near the nucleolus. (c) Enlarged ROI near the edge of nucleus (scale bar: 1 μm)

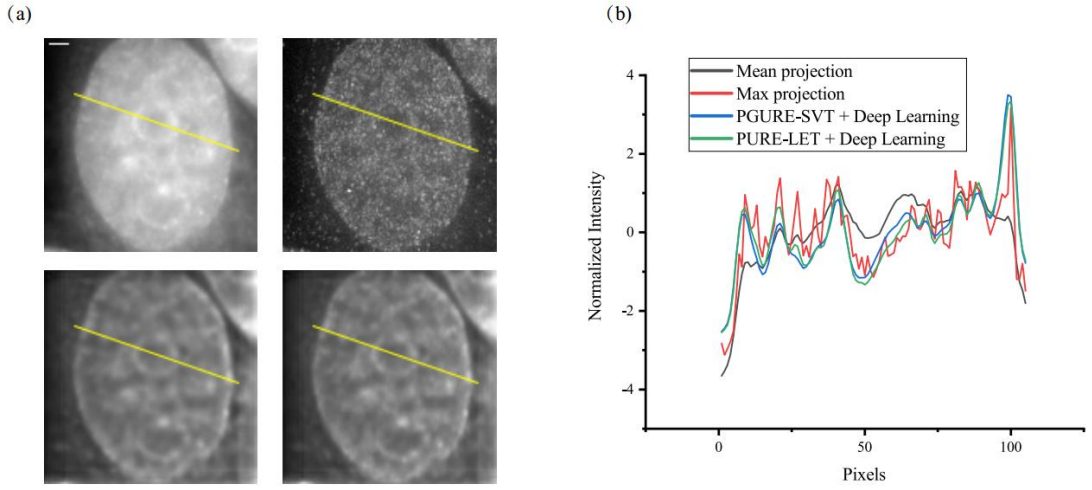

Fig. S6 Comparison between different denoise methods. (a) Upper left: mean projection (scale bar: 2 μm); Upper right: max projection; Lower left: PGURE-SVT (Furnival *et al*. 2017) with deep learning; Lower right: PURE-LET with deep learning. (b) Normalized intensity plots along the yellow lines in (a)

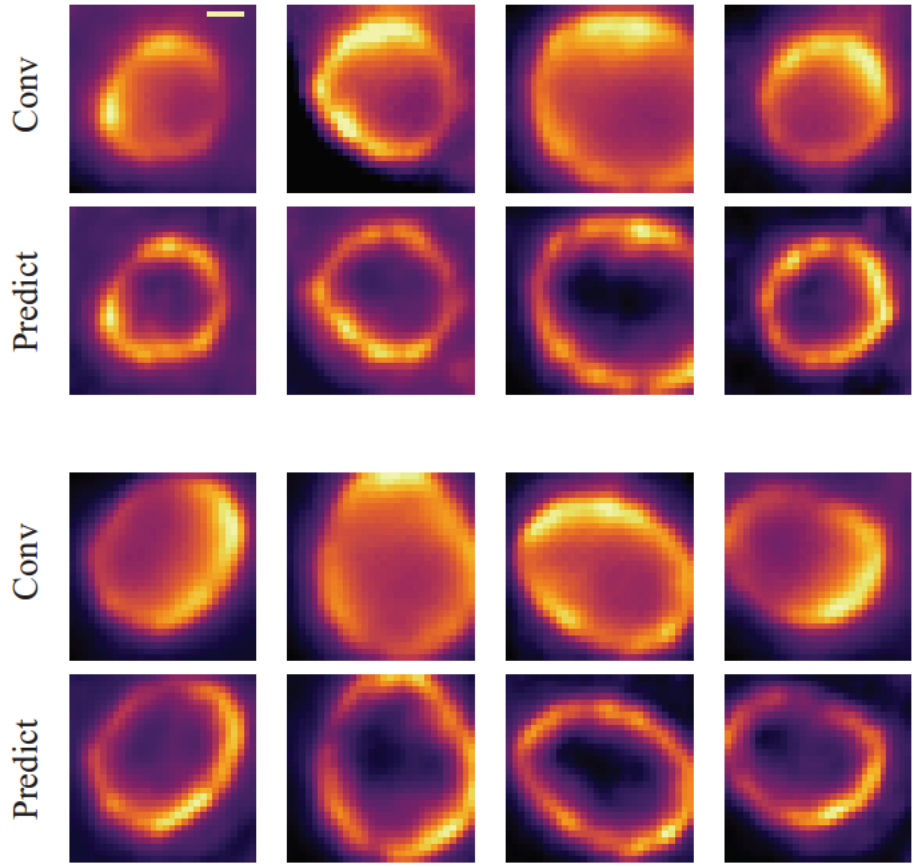

Fig. S7 Generalization performance to fluorescence structure imaging of NCL (scale bar: 1 μm)

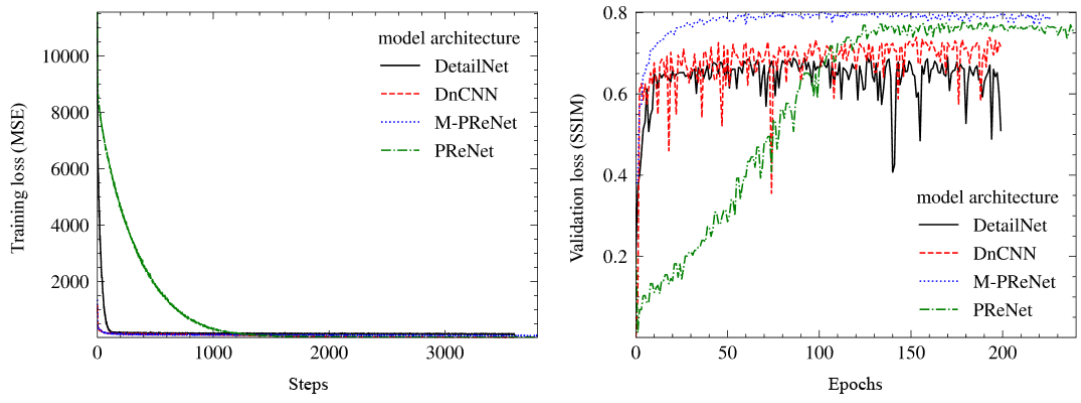

Fig. S8 Training loss (MSE) and validation loss (SSIM) for different methods

Supplementary tables

Table S1 Computational consumption

	Train	Validation
Total epoch	200	200
Sum(s)	172.99327	0.90484
Minimum(s)	0.85436	0.0043
Maximum(s)	1.15472	0.01139
Median(s)	0.8586	0.00438
Mean(s)	0.86497	0.00452
Data size*	(128, 1, 30, 30)	(25, 1, 30, 30)

*Each value corresponds to batch size, channel, width and height

Supplementary movies

This article contains two Supplementary movies.

Reference:
Furnival T, Leary RK, Midgley PA (2017) Denoising time-resolved microscopy image sequences with singular value thresholding. Ultramicroscopy 178:112-124